Supplementary Information

Dinuclear Ir(III) complexes with asymmetrical bridging ligands as highly efficient phosphors for single-layer electroluminescent devices

Hui-Ting Mao,[a] Yang Cui,[a] Guang-Fu Li,[a] Guo-Gang Shan,[a,*] Qun-Ying Zeng,[b,*] Fu-Shan Li,[b] Zhong-Min Su,[a, c*]

[a] *Institute of Functional Material Chemistry and National & Local United Engineering Lab for Power Battery, Faculty of Chemistry, Northeast Normal University, Changchun 130024, P. R. China.* E-mail:shangg187@nenu.edu.cn (G. Shan); zmsu@nenu.edu.cn (Z. Su)

[b] *Institute of Optoelectronic Technology, FuZhou University, FuZhou, 350002, P. R. China.* E-mail: qyzeng@fzu.edu.cn (Q. Zeng)

[c] *Jilin Provincial Science and Technology Innovation Center of Optical Materials and Chemistry, School of Chemistry and Environmental Engineering, Changchun University of Science and Technology Changchun, 130022, P. R. China.*

Table of Contents

Experimental section

General Methods

All reagents and solvents were procured from commercial sources and used without further purification. All reactions were performed under a Ar_2 atmosphere. ^1H NMR spectra were recorded on a Bruker Avance 500 MHz spectrometer with tetramethylsilane (TMS) as an internal standard. Mass spectra data was measured on matrix-assisted laser desorption-ionization time-of-flight (MALDI-TOF) mass spectrometry. UV-vis absorption spectra and PL emission spectra of these dinuclear cationic Ir(III) complexes were recorded on Cary 500 UV-Vis-NIR spectrophotometer and FL-4600 FL spectrophotometer, respectively.

Single Crystal X-Ray Diffraction Analysis

Single crystal of ***s*-DIr1-dfppz** was cultivated from CH_2Cl_2, CH_3OH and ether solutions by slowly evaporating the solutions. The single-crystal X-ray diffraction data for the dinuclear cationic Ir(III) complex was obtained on a Bruker Apex CCD II area-detector diffractometer. The structures were refined by the full-matrix least-square on the SHELXL-97 program.

Theoretical calculations

Theoretical calculations on the ground and excited electronic states of the dinuclear Ir(III) complexes ***s*-DIr1-dfppz**, ***as*-DIr2-dfppz**, and ***as*-DIr3-ppy** were carried out using density functional theory (DFT) at the B3LYP level. A Double-ξ quality basis set containing LANL2DZ was employed for Ir atom, while a 6-31G* basis set for other atoms. Theoretical calculations were performed with the Gaussian 09 software package.

Electrochemical Measurements

Electrochemical measurements of the dinuclear cationic Ir(III) complexes were performed using cyclic voltammetry (CV) and recorded in CH_3CN solution (10^{-3} M) with a scan rate of 100 mV s^{-1}. Tetrabutylammo-nium perchlorate (Bu_4NClO_4) (0.1 M) in CH_3CN was used as the supporting electrolyte and the ferrocene acted as the internal standard. The HOMO/LUMO energy levels and the energy gap (ΔE) of the complexes were calculated from the first oxidation potential (E_{ox}) and first reduction (E_{red}) potential.

Synthesis of L1

2-(pyridin-2-yl)-1*H*-benzo[d]imidazole(6.00 g, 30.73 mmol), K_2CO_3 (4.25 g, 30.73 mmol), and KOH (1.72 g, 30.73 mmol) were dissolved in acetone. After the mixture was stirred and refluxed for 1 h, 1,4-dibromobutane (4.40 mL, 36.88 mmol) in acetone was added and then the mixture was refluxed overnight under Ar_2 atmosphere. The solvent was removed in vacuo and the residue was extracted by CH_2Cl_2, and column chromatography gave the intermediate product (1-(4-bromobutyl)-2-(pyridin-2-yl)-1*H*-benzo[d]imidazole). Then, 2-(pyridin-2-yl)-1*H*-benzo[d]imidazole (1.41 g, 4.27 mmol), K_2CO_3 (0.59 g, 4.27 mmol), and KOH (0.24 g, 4.27 mmol) were added to acetone solution. After the mixture was stirred and refluxed for 1 h, intermediate product (1-(4-bromobutyl)-2-(pyridin-2-yl)-1*H*-benzo[d]imidazole) (1.00 g, 5.12 mmol) in acetone was added and then the mixture was refluxed overnight under Ar_2 atmosphere. The solvent was removed under vacuum and the the resulting solid was extracted with CH_2Cl_2. The organic layer was collected and dried with Na_2SO_4. The solvent was removed in vacuo, and then the residue was purified by silica gel column chromatography to afford a white powder with a yield of 80%. ^{1}H NMR (500 MHz, $CDCl_3$, δ [ppm]): 8.54-8.55 (m, 2H), 8.40 (d, J = 8.0 Hz, 2H), 7.08-7.85 (m, 4H), 7.37-7.38 (m, 2H), 7.26-7.33 (m, 6H), 4.86 (t, J = 7.0 Hz, 4H), 2.01 (t, J = 7.0 Hz, 4H). MS [m/z]: Calcd for $C_{28}H_{24}N_6$: 444.2, Found 444.2 $[M]^+$.

Synthesis of L2 Yield 73%. ^{1}H NMR (500 MHz, $CDCl_3$, δ [ppm]): 8.56-8.61 (m, 2H), 8.39 (d, J = 8.0 Hz, 1H), 8.30-8.32 (m, 1H), 8.16 (d, J = 7.5 Hz, 2H), 7.77-7.84 (m, 3H), 7.39-7.47 (m, 4H), 7.24-7.32 (m, 4H), 4.88-4.92 (m, 4H), 1.99-2.10 (m, 4H). MS [m/z]: Calcd for $C_{29}H_{25}N_7$: 471.2, Found 471.2 $[M]^+$.

Synthesis of *s*-DIr1-dfppz. dfppz (2.52 g, 14.00 mmol) and $IrCl_3 \cdot 3H_2O$ (2.12 g, 6.00 mmol) were added to a 250 mL round-necked flask. Then 2-ethoxyethanol (120 mL) and water (40 mL) were added to the flask sequentially. The mixture was refluxed for 24 h under Ar_2 atmosphere. After cooling, the resulting precipitate was collected by filtration and washed with water and enthanol. The dried chloro-bridged dimer (0.58 g, 0.50 mmol) and **L1** (0.20 g, 0.45 mmol) in ethylene glycol were heated to 150 °C for 12 h under Ar_2 in the dark. After cooling to room temperature, the reaction mixture was poured into saturated aqueous NH_4PF_6 solution, resulting in a green suspension. The suspension was filtered and extracted with CH_2Cl_2. The crude product was purified by silica gel column chromatography using $CH_3COOC_2H_5$:CH_2Cl_2 in 1:1 (v:v) ratio as the eluent to afford the desired Ir(III) complex. Yield 75%. ^{1}H NMR (500 MHz, d_6-DMSO,

ppm):δ 8.59-8.67 (m, 4H), 8.58 (d, *J* = 3.0 Hz, 2H), 8.28-8.33 (m, 2H), 8.20 (d, *J* = 5.0 Hz, 2H), 7.95 (t, *J* = 7.5 Hz, 2H), 7.73-7.77 (m, 2H), 7.46-7.50 (m, 2H), 7.26-7.29 (m, 4H), 7.14-7.23 (m, 6H), 6.72-6.75 (m, 4H), 6.36 (d, *J* = 8.0 Hz, 2H), 5.68-5.71 (m, 4H), 4.92-4.95 (m, 4H), 2.16-2.20 (m, 4H). MS [m/z]: Calcd for $C_{64}H_{44}F_{20}Ir_2N_{14}P_2$: 1836.2, Found 1836.2 $[M]^+$. Anal. Calcd for $C_{64}H_{44}F_{20}Ir_2N_{14}P_2$: C, 41.88; H, 2.42; N, 10.68. Found: C, 41.82; H, 2.39; N, 10.72.

Synthesis of *as*-DIr2-dfppz. Yield 66%. ^{1}H NMR (500 MHz, d_6-DMSO, ppm):δ 8.69-8.71 (m, 1H), 8.65 (s, 1H), 8.58-8.63 (m, 2H), 8.56 (s, 1H), 8.49 (d, *J* = 2.5 Hz, 1H), 8.37 (t, *J* = 8.0 Hz, 1H), 8.26-8.32 (m, 1H), 8.15-8.18 (m, 1H), 8.01 (t, *J* = 8.0 Hz, 2H), 7.68-7.76 (m, 3H), 7.37-7.45 (m, 2H), 7.15-7.24 (m, 6H), 7.10-7.13 (m, 1H), 6.98-7.03 (m, 2H), 6.85-6.87 (m, 1H), 6.74-6.82 (m, 3H), 6.63-6.68 (m, 2H), 6.59-6.62 (m, 1H), 6.36 (m, 1H), 5.65 (t, *J* = 6.5 Hz, 2H), 5.56 (t, *J* = 5.0 Hz, 1H), 5.05 (d, *J* = 7.5 Hz, 3H), 4.84-4.92 (m, 2H), 2.12-2.50 (m, 4H). MS [m/z]: Calcd for $C_{65}H_{45}F_{20}Ir_2N_{15}P_2$: 1863.2, Found 1863.2 $[M]^+$. Anal. Calcd for $C_{65}H_{45}F_{20}Ir_2N_{15}P_2$: C, 41.92; H, 2.44; N, 11.28. Found: C, 41.85; H, 2.48; N, 11.25.

Synthesis of *as*-DIr3-ppy. Yield 72%. ^{1}H NMR (500 MHz, d_6-DMSO, ppm):δ 8.71 (t, *J* = 9.5 Hz, 1H), 8.58 (t, *J* = 9.0 Hz, 1H), 8.33 (t, *J* = 8.0 Hz, 1H), 8.28 (d, *J* = 8.5 Hz, 2H), 8.23 (t, *J* = 8.0 Hz, 2H), 8.14 (m, 1H), 7.98 (s, 2H), 7.88-7.95 (m, 5H), 7.86 (t, *J* = 8.5 Hz, 1H), 7.78-7.82 (m, 2H), 7.70-7.76 (m, 3H), 7.60-7.69 (m, 3H), 7.33-7.39 (m, 2H), 7.21-7.27 (m, 1H), 6.96-7.13 (m, 7H), 6.87-6.92 (m, 5H), 6.78-6.85 (m, 3H), 6.65 (t, *J* = 7.5 Hz, 1H), 6.56-6.61 (m, 1H), 6.25 (d, *J* = 8.0 Hz, 1H), 6.20 (m, 2H), 6.03 (t, *J* = 8.0 Hz, 1H), 5.85-5.88 (m, 1H), 5.04 (s, 2H), 4.86 (m, 2H), 2.06-2.19 (m, 4H). MS [m/z]: Calcd for $C_{73}H_{57}F_{12}Ir_2N_{11}P_2$: 1761.3, Found 1761.3 $[M]^+$. Anal. Calcd for $C_{73}H_{57}F_{12}Ir_2N_{11}P_2$: C, 49.74; H, 3.26; N, 8.74. Found: C, 49.69; H, 3.21; N, 8.78.

Synthesis of $(dfppz)_2$IrL1: Yield 76%. ^{1}H NMR (600 MHz, DMSO-d_6, δ [ppm]): 8.80 (d, *J* = 12.0 Hz, 1H), 8.64 (d, *J* = 6.0 Hz, 1H), 8.60 (d, *J* = 3.0 Hz, 1H), 8.34-8.37 (m, 1H), 8.16 (d, *J* = 6.0 Hz, 1H), 8.00 (d, *J* = 6.0 Hz, 1H), 7.73 (t, *J* = 6.0 Hz, 1H), 7.49 (t, *J* = 6.0 Hz, 1H), 7.26 (d, *J* = 6.0 Hz, 2H), 7.12-7.22 (m, 3H), 6.73-6.74 (m, 2H), 6.35 (d, *J* = 12.0 Hz, 1H), 5.70-5.73 (m, 2H), 4.47 (s, 3H). MS (MALDI-TOF): m/z 760.2 (M-PF_6).

Synthesis of $(dfppz)_2$IrL2: Yield 65%. ^{1}H NMR (600 MHz, DMSO-d_6, δ [ppm]): 8.63-8.66 (m, 2H), 8.52 (d, *J* = 2.4 Hz, 1H), 8.38 (t, *J* = 6.0 Hz, 1H), 8.02 (d, *J* = 6.0 Hz, 1H), 7.81 (d, *J* = 1.8 Hz, 1H), 7.74 (t, *J* = 6.0 Hz, 1H), 7.35 (s, 1H), 7.26 (t, *J* = 12.0

Hz, 1H), 7.01-7.11 (m, 3H), 7.00 (d, J = 6.0 Hz, 2H), 6.84 (t, J = 6.0 Hz, 1H), 6.81 (t, J = 6.0 Hz, 1H), 6.64-6.68 (m, 1H), 5.57 (d, J = 6.0 Hz, 1H), 5.07 (d, J = 6.0 Hz, 1H), 4.53 (s, 3H). MS (MALDI-TOF): m/z 787.1 (M-PF_6).

Synthesis of $(ppy)_2$IrL1: Yield 80%. ^{1}H NMR (600 MHz, DMSO-d_6, δ [ppm]): 8.78 (d, J = 6.0 Hz, 1H), 8.25-8.31 (m, 2H), 8.19 (d, J = 12.0 Hz, 1H), 7.90-7.97 (m, 5H), 7.86 (t, J = 12.0 Hz, 1H), 7.69-7.71 (m, 2H), 7.63 (d, J = 6.0 Hz, 1H), 7.42 (t, J = 12.0 Hz, 1H), 7.10-7.15 (m, 2H), 7.06 (t, J = 12.0 Hz, 1H), 7.01-7.04 (m, 2H), 6.90-6.94 (m, 2H), 6.29 (d, J = 12.0 Hz, 1H), 6.19-6.22 (m, 2H), 4.46 (s, 3H). MS (MALDI-TOF): m/z 710.2 (M-PF_6).

Synthesis of $(ppy)_2$IrL2: Yield 78%. ^{1}H NMR (600 MHz, DMSO-d_6, δ [ppm]): 8.64 (d, J = 12.0 Hz, 1H), 8.29-8.33 (m, 2H), 8.25 (d, J = 6.0 Hz, 1H), 8.02 (d, J = 12.0 Hz, 1H), 7.96 (t, J = 6.0 Hz, 1H), 7.84-7.91 (m, 2H), 7.79 (d, J = 5.4 Hz, 1H), 7.69 (t, J = 12.0 Hz, 1H), 7.64 (d, J = 6.0 Hz, 1H), 7.44 (d, J = 6.0 Hz, 1H), 7.27 (t, J = 12.0 Hz, 1H), 7.11-7.15 (m, 4H), 6.98 (t, J = 12.0 Hz, 1H), 6.89 (t, J = 6.0 Hz, 2H), 6.84 (t, J = 12.0 Hz, 1H), 6.68 (t, J = 6.0 Hz, 1H), 6.59 (t, J = 12.0 Hz, 1H), 6.04 (d, J = 6.0 Hz, 1H), 5.87 (d, J = 6.0 Hz, 1H), 4.53 (s, 3H). MS (MALDI-TOF): m/z 737.2 (M-PF_6).

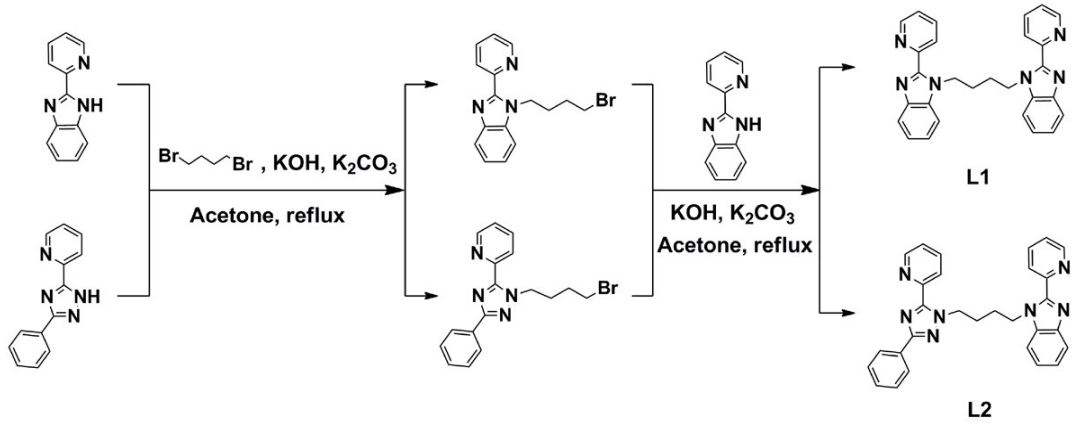

Scheme S1. Synthetic routes of **L1** and **L2**.

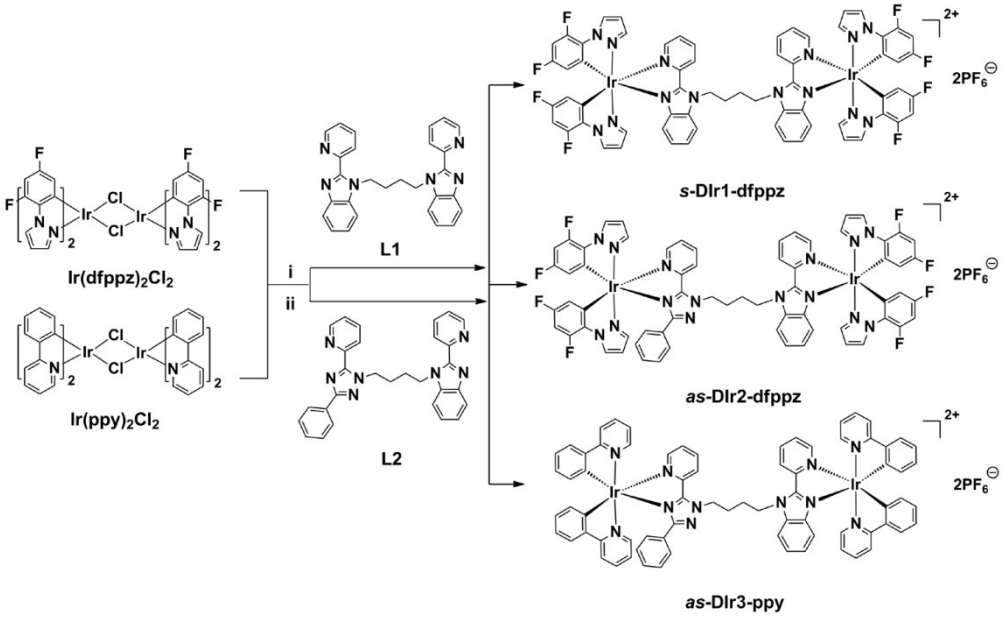

Scheme S2. Synthetic routes of ***s*-DIr1-dfppz**, ***as*-DIr2-dfppz**, and ***as*-DIr3-ppy**. (i) ethylene glycol, 150 °C, 12 h; (ii) aqueous NH_4PF_6 solution.

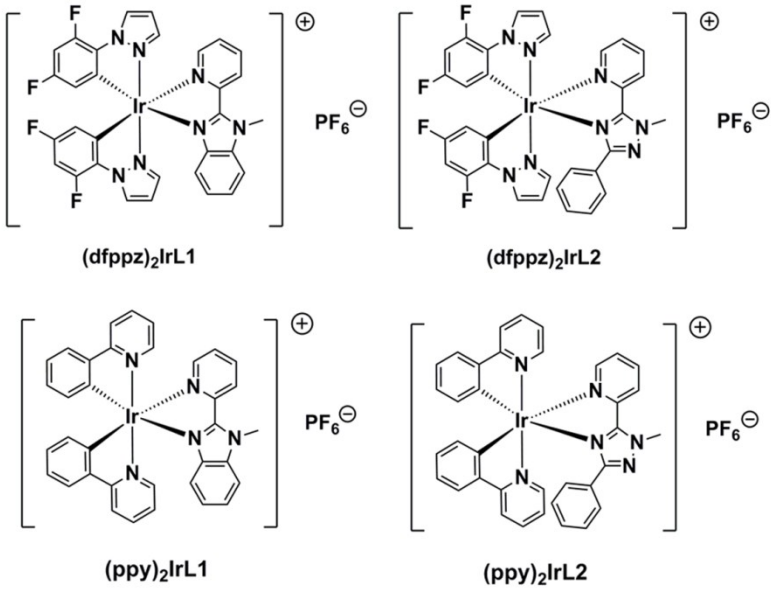

Scheme S3. Chemical structures of the mononuclear Ir(III) complexes.

Table S1. Photophysical properties of the mononuclear Ir(III) complexes.

Complexes	$\lambda_{PL,max}$[a,b] [nm]	Φ_p[a,b] [%]	τ[a,b] [μs]
$(dfppz)_2IrL1$	525, 513	51, 77	2.91, 3.90
$(dfppz)_2IrL2$	502, 484	27, 65	2.25, 1.85
$(ppy)_2IrL1$	571, 570	28, 40	2.44, 1.90
$(ppy)_2IrL2$	573, 553	13, 15	7.38, 1.94

[a] In CH_3CN at 298 K. [b] In neat film at 298 K.

Table S2. Crystal data and structure refinement of ***s*-DIr1-dfppz**.

Name	***s*-DIr1-dfppz**
Identification code	CCDC 1901587
Formula	$C_{64}H_{44}F_{20}Ir_2N_{14}P_2$
Formula weight	1835.47
Crystal system	Triclinic
Space group	P-1
Cell Lengths (Å)	a 9.0935(6) b 13.5384(10) c 16.5246(11)
Cell Angles (°)	α 66.373(3) β 79.409(3) γ 75.388(3)
Cell Volume ($Å^3$)	1795.7(2)
Z	1
$D_{calcd.}$(g m^{-3})	1.697
F(000)	890.0
R_{int}	0.0833
Goodness-of-fit on F^2	1.083
R_1[a], wR_2[b] [I>=2σ (I)]	0.0557, 0.1185
R_1, wR_2 [all data]	0.0791, 0.1312

[a] $R_1 = \Sigma||F_o|- |F_c||/\Sigma|F_o|$. [b] $wR_2 = |\Sigma w(|F_o|^2-|F_c|^2)|/\Sigma|w(F_o^2)^2|^{1/2}$.

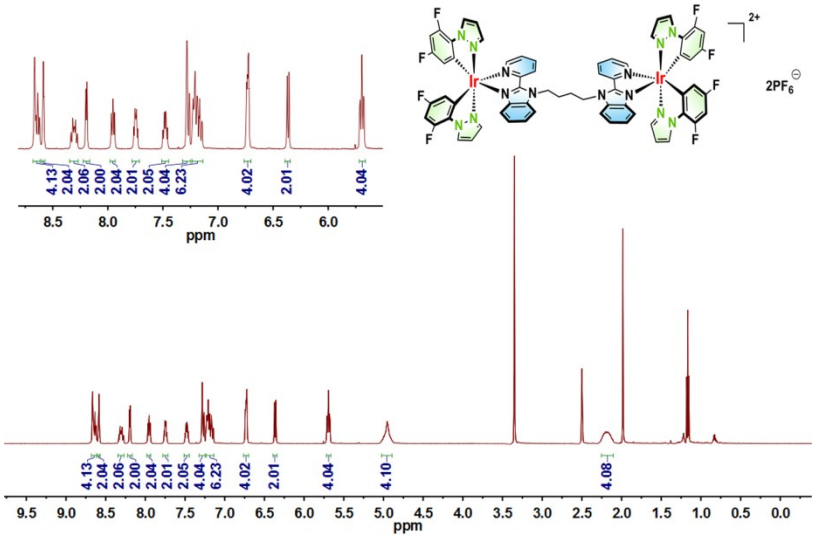

Figure S1. ^{1}H NMR spectrum of ***s*-DIr1-dfppy** in DMSO-d_6.

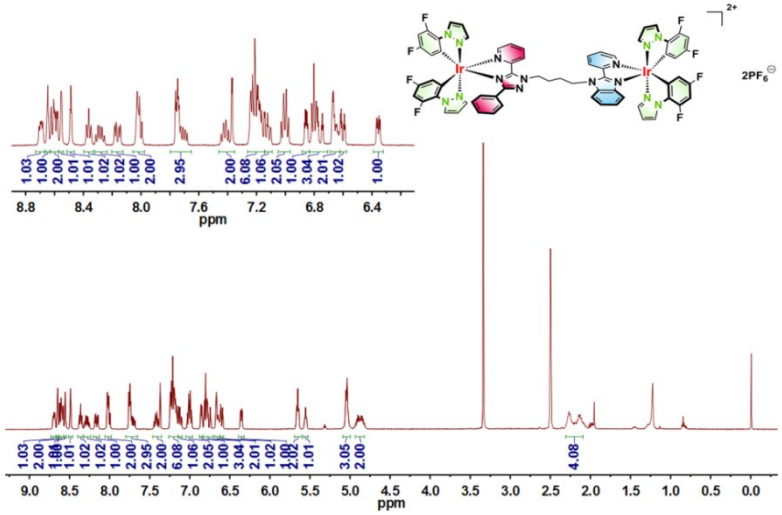

Figure S2. ^{1}H NMR spectrum of ***as*-DIr2-dfppy** in DMSO-d_6.

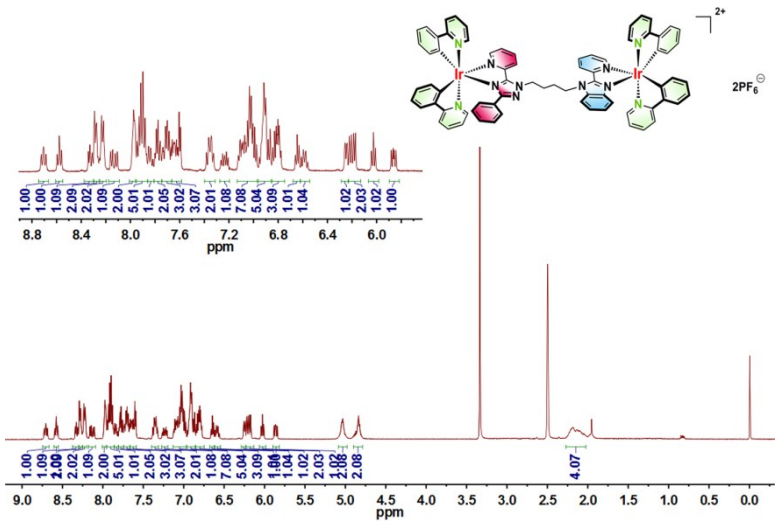

Figure S3. ^{1}H NMR spectrum of ***as*-DIr3-ppy** in DMSO-d_6.

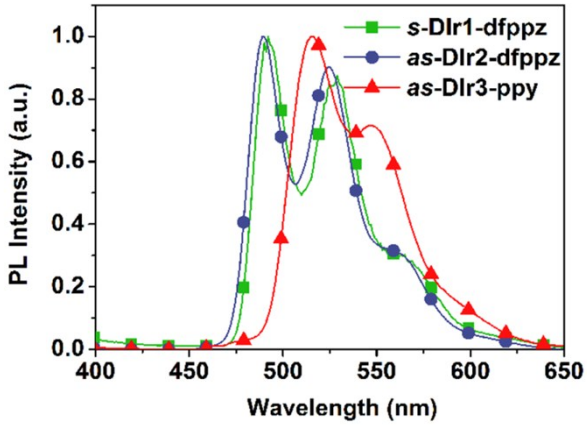

Figure S4. PL spectra of the dinuclear Ir(III) complexes at 77 K.

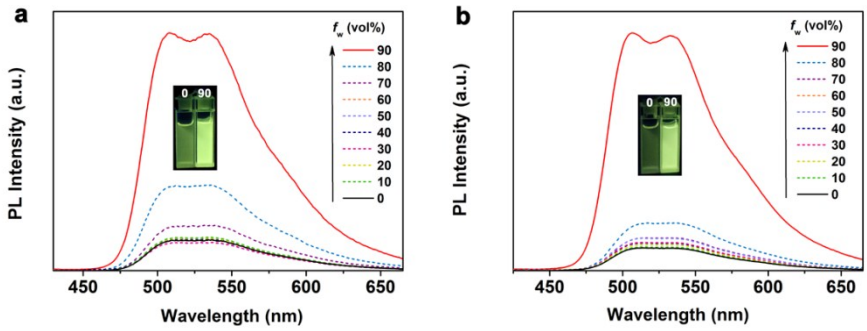

Figure S5. a) PL spectra of ***s*-DIr1-dfppz** in CH_3CN/water mixtures with different water fractions (f_w). Inset: photos of ***s*-DIr1-dfppz** in CH_3CN/water mixtures (f_w = 0 and 90%). b) PL spectra of ***as*-DIr2-dfppz** in CH_3CN/water mixtures. Inset: photos of ***as*-DIr2-dfppz** in CH_3CN/water mixtures (f_w = 0 and 90%).

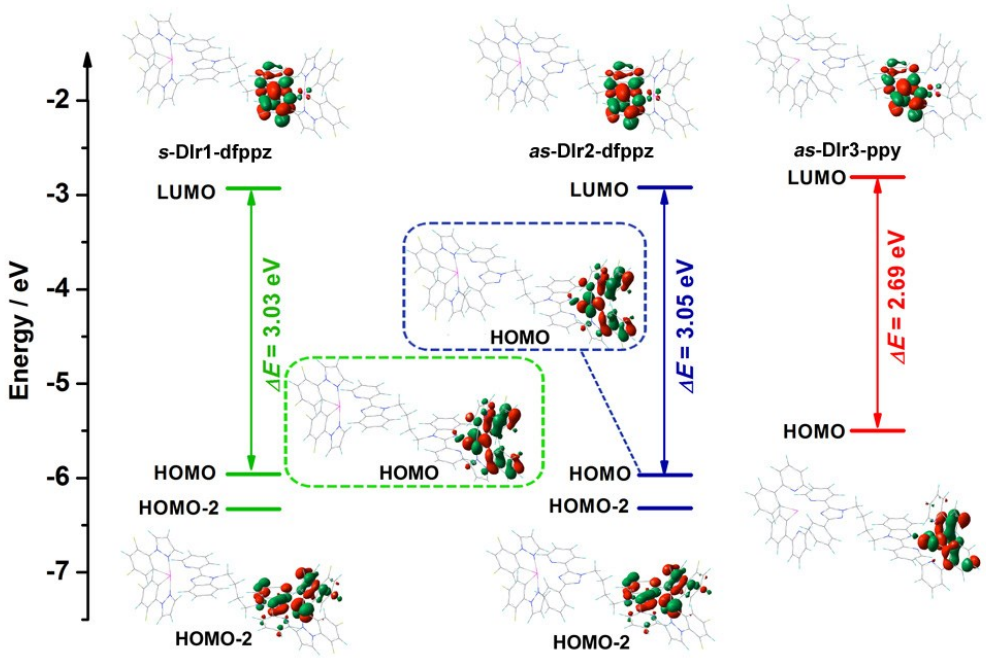

Figure S6. Electron density contours (0.04 e·bohr^{-3}) calculated for HOMOs and LUMOs of ***s*-DIr1-dfppz**, ***as*-DIr2-dfppz**, and ***as*-DIr3-ppy**. HOMO-2 involved in the excitations for complexes ***s*-DIr1-dfppz** and ***as*-DIr2-dfppz** are also shown.

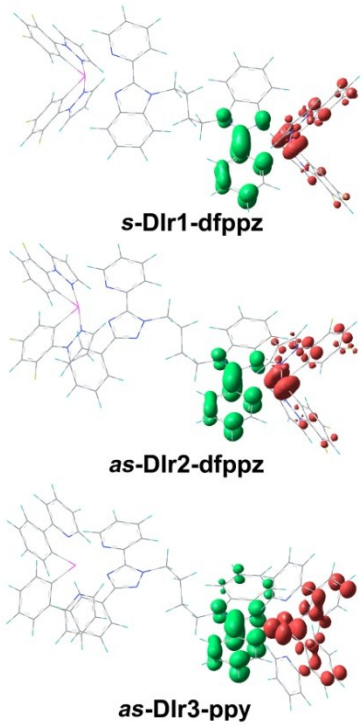

Figure S7. Difference electron density (0.003 e·bohr^{-3}) computed by subtracting the electron densities of the T_1 and S_0 states for ***s*-DIr1-dfppz**, ***as*-DIr2-dfppz**, and ***as*-DIr3-ppy**. The charge goes from the red to the green areas.

Table S3. Calculated energy levels, oscillator strengths, and orbital transition analyses of T_1 states for ***s*-DIr1-dfppz**, ***as*-DIr2-dfppz**, and ***as*-DIr3-ppy**.

Complex	State	eV	*f*	Assignment[a]	Character
***s*-DIr1-dfppz**	T_1	2.16	0.00	H→L (45%)	^{3}MLCT/^{3}LLCT
				H-2→L (42%)	^{3}MLCT/^{3}LLCT/^{3}ILCT
***as*-DIr2-dfppz**	T_1	2.15	0.00	H→L (44%)	^{3}MLCT/^{3}ILCT
				H-2→L (43%)	^{3}MLCT/^{3}LLCT/^{3}ILCT
***as*-DIr3-ppy**	T_1	1.99	0.00	H→L (99%)	^{3}MLCT/^{3}LLCT

[a] H and L denote the highest occupied molecular orbital (HOMO) and the lowest unoccupied molecular orbital (LUMO), respectively.

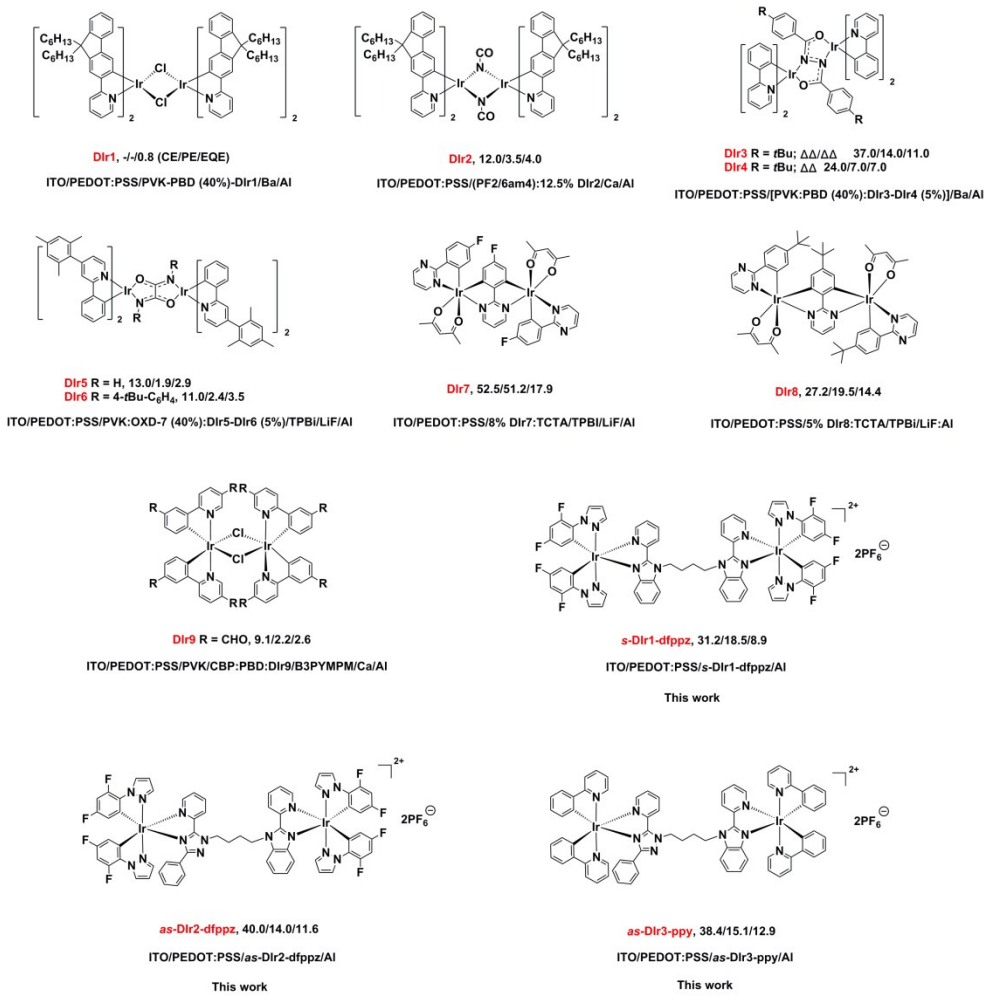

Figure S8. Chemical structures of the dinuclear Ir(III) complexes and the corresponding performances of solution-processed devices in reported works.

Table S4. Summary of representative performances of solution-processed devices based on dinuclear Ir(III) complexes in reported works.

Complex	$V_{turn\text{-}on}$[a] (V)	$\lambda_{max,em}$ (nm)	L_{max}[b] (cd m^{-2})	CE[c] (cd A^{-1})	PE[d] (lm W^{-1})	EQE[e] (%)	CIE[f]	Previous report
DIr1 (multilayer doped)	-	550	13000	-	-	0.8	-	Ref [S1][1]
DIr2 (multilayer doped)	7.5	546	670	12.0	3.5	4.0	-	Ref [S2][2]
DIr3 (multilayer doped)	5.5	526	7000	37.0	14.0	11.0	-	Ref [S3][3]
DIr4 (multilayer doped)	6.2	526	11000	24.0	7.0	7.0	-	Ref [S3]
DIr5 (multilayer doped)	-	533	25400	13.0	1.9	2.9	(0.34, 0.63)	Ref [S4][4]
DIr6 (multilayer doped)	-	533	25630	11.0	2.4	3.5	(0.34, 0.62)	Ref [S4]
DIr7 (multilayer doped)	3.2	564	46206	52.5	51.2	17.9	-	Ref [S5][5]
DIr8 (multilayer doped)	3.1	598	18410	27.2	19.5	14.4	(0.56, 0.44)	Ref [S6][6]
DIr9 (multilayer doped)	7.7	551	>6000	9.1	2.2	2.6	(0.44, 0.54)	Ref [S7][7]
s-DIr1-dfppz	3.0	518	6475	31.2	18.5	8.9	(0.39, 0.57)	This work
as-DIr2-dfppz	2.7	517	3368	40.0	14.0	11.6	(0.39, 0.57)	This work
as-DIr3-ppy	4.3	580	2558	38.4	15.1	12.9	(0.55, 0.44)	This work

[a] The turn on voltage estimated at 1 cd m^{-2}; [b] The maximum luminance; [c] Maximum CE values; [d] Maximum PE values; [e] Maximum EQE values; [f] CIE coordinates.

1 S. Bettington, M. Tavasli, M. R. Bryce, A. S. Batsanov, A. L. Thompson, H. A. Al Attar, F. B. Dias and A. P. Monkman, *J. Mater. Chem.*, 2006, **16**, 1046-1052.

2 A. M'Hamedi, A. S. Batsanov, M. A. Fox, M. R. Bryce, K. Abdullah, H. A. Al-Attar and A. P. Monkman, *J. Mater. Chem.*, 2012, **22**, 13529-13540.

3 Y. Zheng, A. S. Batsanov, M. A. Fox, H. A. Al-Attar, K. Abdullah, V. Jankus, M. R. Bryce and A. P. Monkman, *Angew. Chem., Int. Ed.* , 2014, **53**, 11616-11619.

4 A. M'hamedi, M. A. Fox, A. S. Batsanov, H. A. Al-Attar, A. P. Monkman and M. R. Bryce, *J. Mater. Chem. C*, 2017, **5**, 6777-6789.

5 X. Yang, Z. Feng, J. Zhao, J.-S. Dang, B. Liu, K. Zhang and G. Zhou, *ACS Appl. Mater. Interfaces*, 2016, **8**, 33874-33887.

6 X. Yang, X. Xu, J. S. Dang, G. Zhou, C. L. Ho and W. Y. Wong, *Inorg. Chem.*, 2016, **55**, 1720-1727.

7 M. Y. Wong, G. Xie, C. Tourbillon, M. Sandroni, D. B. Cordes, A. M. Slawin, I. D. Samuel and E. Zysman-Colman, *Dalton Trans.*, 2015, **44**, 8419-8432.